PAPER

Ratiometric fluorescence sensing of D-allulose using an inclusion complex of γ-cyclodextrin with a benzoxaborole-based probe†

Yota Suzuki, [ID] * Takeshi Hashimoto [ID] and Takashi Hayashita [ID] *

Because D-allulose has been attracting attention as a zero-calorie sugar, the selective sensing of D-allulose is desired to investigate its health benefits. We report herein a novel fluorescence chemosensor that is based on an inclusion complex of γ-cyclodextrin (γ-CyD) with a benzoxaborole-based probe. Two inclusion complexes, **1/γCyD** and **2/γCyD**, were prepared by mixing γ-CyD with their corresponding probes in a water-rich solvent, where γ-CyD encapsulates two molecules of the probes inside its cavity to form a pyrene dimer. Both **1/γCyD** and **2/γCyD** exhibit monomeric and dimeric fluorescence from the pyrene moieties. By the reaction of **1/γCyD** with saccharides, the intensities of monomeric and dimeric fluorescence remained unchanged and decreased, respectively. We have demonstrated that **1/γCyD** has much higher affinity for D-allulose than for the other saccharides (D-fructose, D-glucose, and D-galactose). The conditional equilibrium constants for the reaction systems were determined to be 498 ± 35 M^{-1} for D-fructose, 48.4 ± 25.3 M^{-1} for D-glucose, 15.0 ± 3.3 M^{-1} for D-galactose, and $(8.05 \pm 0.59) \times 10^3$ M^{-1} for D-allulose. These features of **1/γCyD** enable ratiometric fluorescence sensing with high sensitivity and selectivity for D-allulose. The limits of detection and quantification of **1/γCyD** for D-allulose at pH 8.0 were determined to be 6.9 and 21 μM, respectively. Induced circular dichroism spectral study has shown that the reaction of **1/γCyD** with D-allulose causes the monomerisation of the dimer of probe **1** that is encapsulated by γ-CyD, which leads to the diminishment of the dimeric fluorescence.

Introduction

Because modern diets are centred on high-calorie foods, the number of people with diabetes is increasing worldwide.[1] It is estimated that the total number of diabetic patients will exceed 300 million, making diabetes the seventh leading cause of death in 2030.[2,3] Therefore, the promotion of healthy eating habits is an urgent issue to prevent diabetes. Recently, D-allulose, a rare sugar, has been attracting attention for the following health benefits: it has almost zero calories (0.2 kcal g^{-1}) and its sweetness is 70% of that of sucrose; it hardly accumulates in the body;[4,5] and it has strong anti-hyperlipidemic and anti-hyperglycemic effects.[6] Such beneficial features are appealing to researchers in medicine and biology who are engaged in tackling global health issues.

A boronic acid molecule in aqueous solution forms an sp2 trigonal boronic acid and an sp3 tetrahedral boronate ion on the acidic and basic sides of its pK_a (pK_a^B), respectively. Boronic acids react rapidly with saccharides to form tetrahedral boronate ester ions, and this property has enabled the development of boronic acid-based saccharide chemosensors.[7–9] It is well known that boronic acids react with D-fructose selectively; however, it has been recently reported that D-allulose has higher affinity for boronic acids than D-fructose.[10,11] In particular, *ortho*-hydroxymethyl phenylboronic acid cyclic monoester (benzoxaborole, p$K_a^B = 7.34$)[12] shows 12 times larger binding constant in the reaction with D-allulose than D-fructose, reported by Arimitsu *et al.*[11] Hence, using benzoxaborole as the reaction site is expected to enable highly sensitive and selective sensing of D-allulose.

We have reported various inclusion complexes of cyclodextrins with boronic acid-based probes, which can recognise saccharides in a water-rich solvent.[13] Among them, the inclusion complex of γ-cyclodextrin (γ-CyD) with a pyrene-introduced probe exhibits two types of emission, monomeric and dimeric fluorescence, and the ratio of the fluorescence intensities changes depending on the saccharide concentration.[14] Such fluorescence response enables ratiometric sensing of saccharides and realises reliable analysis that avoids the effects of the surrounding environment, *e.g.*, temperature and polarity, on the emission intensity.[15]

Department of Materials and Life Sciences, Faculty of Science and Technology, Sophia University, 7-1, Kioi-cho, Chiyoda-ku, Tokyo, 102-8554, Japan. E-mail: y-suzuki-3k3@sophia.ac.jp; ta-hayas@sophia.ac.jp

In this study, we synthesised a novel boronic acid-based probe possessing benzoxaborole and pyrene moieties, **1** in Scheme 1, and evaluated the features of the ratiometric fluorescence response of the inclusion complex of **1** with γ-CyD to D-allulose in a water-rich solvent of dimethyl sulfoxide (DMSO)/water (2/98 in v/v). By exploiting various spectrophotometric techniques, we investigated the affinity of the inclusion complex for saccharides (D-allulose, D-fructose, D-glucose, and D-galactose) and the sensing mechanism. We also evaluated a *para*-substituted analogue, **2**, as a saccharide chemosensor, and elucidated the effect of the probe structure on saccharide recognition.

Experimental

Materials and instruments

All reagents and organic solvents were used as received from commercial resources without further purification. 1,3-dihydro-1-hydroxy-2,1-benzoxaborole-5-carboxylic acid (**2-COOH**) was synthesised according to the literature method (Scheme S1†).[16] Milli-Q water was used for spectroscopic measurements.

^{1}H and ^{13}C nuclear magnetic resonance (NMR) spectra were acquired with a JEOL JNM-ECA 500 spectrometer (JEOL, Japan) at room temperature. High resolution electrospray ionization mass spectra (ESI-HRMS) were measured using a JEOL The Accu-TOF JMS T100LC (JEOL, Japan). The pH of solutions was measured by a HORIBA pH electrode 9618S-10D connected to a HORIBA pH meter F-52 (Horiba, Japan). UV-vis absorption spectra were obtained at 25 °C using a Hitachi U-3900H spectrophotometer (Hitachi, Japan) equipped with a temperature controller (Hitachi, Japan). Fluorescence spectra were recorded at 25 °C using a Hitachi F-7000 fluorescence spectrophotometer (Hitachi, Japan) equipped with a temperature controller (Hitachi, Japan) and an EYELA CCA-1111 (EYELA, Japan). Induced circular dichroism spectra were recorded at 25 °C using a JASCO J-820 spectrophotometer (JASCO, Japan) equipped with a Peltier

temperature controller (JASCO, Japan) and an EYELA Cool Ace CA-1111 (EYELA, Japan) under a nitrogen atmosphere.

Synthesis of probes

Synthesis of 1. 1,3-dihydro-1-hydroxy-2,1-benzoxaborole-6-carboxylic acid (**1-COOH**, 27 mg, 0.15 mmol) and 1-aminopyrene (35 mg, 0.16 mmol) were dissolved in methanol (5 mL). The solution was stirred for 15 minutes at room temperature subsequently DMT-MM (71 mg, 0.26 mmol) was added with stirring. The mixture was stirred for 3 days at room temperature. The precipitated solid was collected by filtration and washed with excess water and methanol. Yield: 52 mg (91%, light yellow solid), ^{1}H NMR (500 MHz, DMSO-d$_6$, ppm): δ_H 10.85 (s, 1H), 9.40 (s, 1H), 8.54 (s, 1H), 8.36–8.21 (m, 9H), 8.10 (t, $J = 7.4$ Hz, 1H), 7.64 (d, $J = 8.0$ Hz, 1H), 5.13 (s, 2H). ^{13}C NMR (125 MHz, DMSO-d$_6$, ppm): δ_C 166.8, 157.4, 133.5, 132.0, 130.8, 130.5, 130.5, 130.2, 128.9, 127.3, 127.2, 126.9, 126.5, 125.6, 125.3, 125.1, 125.1, 124.9, 124.4, 123.8, 123.0, 121.5, 70.1. A peak of the carbon atom bonding directly to the boron atom was unobserved. ESI-HRMS (neg.) m/z: $[M + 2MeOH - H_2O - H^+]^-$, calcd for $C_{26}H_{21}BNO_4$, 422.15636; found, 422.15306.
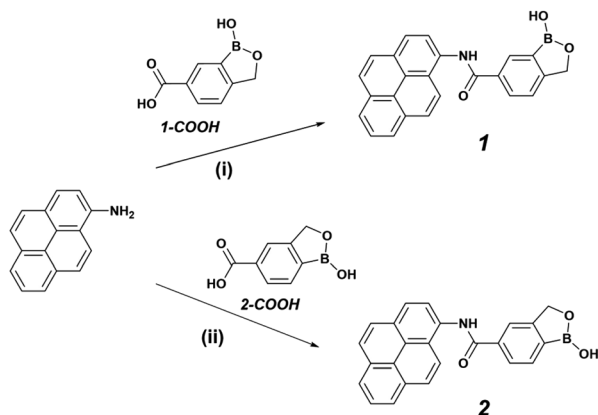
Synthesis of 2. **2-COOH** (60 mg, 0.34 mmol) and 1-aminopyrene (72 mg, 0.33 mmol) were dissolved in methanol (10 mL). The solution was stirred for 15 minutes at room temperature subsequently DMT-MM (0.143 g, 0.52 mmol) was added with stirring. The mixture was stirred for 16 hours at room temperature. The precipitated solid was collected by filtration and washed with excess water and methanol. Yield: 62 mg (50%, yellowish green solid), ^{1}H NMR (500 MHz, DMSO-d$_6$, ppm): δ_H 10.88 (s, 1H), 9.42 (s, 1H), 8.33 (m, 3H), 8.27–8.19 (m, 6H), 8.14–8.08 (m, 2H), 7.94 (d, $J = 7.4$ Hz, 1H), 5.15 (s, 2H). ^{13}C NMR (125 MHz, DMSO-d$_6$, ppm): δ_C 166.6, 154.1, 136.6, 131.8, 130.8, 130.6, 130.5, 129.0, 127.3, 127.2, 127.0, 126.5, 126.5, 125.6, 125.4, 125.1, 125.1, 124.9, 124.4, 123.8, 122.9, 120.9, 70.1. A peak of the carbon atom bonding directly to the boron atom was unobserved. ESI-HRMS (neg.) m/z: $[M + 2MeOH - H_2O - H^+]^-$, calcd for $C_{26}H_{21}BNO_4$, 422.15636; found, 422.15564.

Preparation of sample solutions

Ionic strength of sample solutions was adjusted to 0.10 M with sodium chloride. Solution pH was adjusted with diluted aqueous solutions of hydrochloric acid and 50% sodium hydroxide solution in the presence of 10 mM of phosphate buffer. After dissolving sodium chloride, phosphate salt, cyclodextrin, and saccharide into a mixed solvent of DMSO/water and pH adjustment, an appropriate amount of 1 mM probe DMSO solution was added into the solution with stirring to prepare 10 μM probe solution of DMSO/water (2/98 in v/v).

Spectral measurements under various pH conditions

UV-vis and fluorescence spectra were measured at various pH values by titrating an HCl aq. into a basic sample solution (*ca.* pH 10.5). The solution pH was decreased until *ca.* 4. After each titration, the solution was stirred for 5 minutes subsequently the UV-vis absorption and fluorescence spectra were measured.

Scheme 1 Syntheses of **1** and **2**. (i) DMT-MM, methanol, room temperature, 3 days, 91%, (ii) DMT-MM, methanol, room temperature, 1 day, 50%. DMT-MM = 4-(4,6-dimethoxy-1,3,5-triazin-2-yl)-4-methylmorpholinium chloride.

Spectral measurements under various saccharide concentrations

A series of sample solutions containing various saccharide concentrations (0–30 mM) with sodium chloride, phosphate salt, and cyclodextrin were prepared individually. Each solution was stirred for 5 minutes after the addition of 1 mM probe DMSO solution, subsequently the UV-vis absorption, fluorescence, and induced circular dichroism spectra were measured.

Determination of acid dissociation constants

pH dependence of absorbance at a specific wavelength was analysed using Igor Pro program according to a theoretical sigmoidal curve derived from the acid dissociation model of monobasic acid.

Determination of conditional equilibrium constants

Ratio in fluorescence intensities at 430 and 500 nm (I_{500}/I_{430}) was recorded at various saccharide concentrations. The data were analysed using Igor Pro program according to the theoretical equation derived from the 1 : 1 binding model shown in eqn (1):[17]

$$R = R_0 + \frac{R_{\text{lim}} - R_0}{2C_{\text{probe}}} \left\{ C_{\text{probe}} + C_{\text{sugar}} + \frac{1}{K'} \right.$$
$$\left. - \left[\left(C_{\text{probe}} + C_{\text{sugar}} + \frac{1}{K'} \right)^2 - 4C_{\text{probe}} \times C_{\text{sugar}} \right]^{\frac{1}{2}} \right\} \quad (1)$$

where C_{sugar} is the total concentration of saccharide; R and R_0 represent the value of I_{500}/I_{430} in the presence and absence of saccharide, respectively; R_{lim} is the value of R when the change of R reaches saturation; K' is the conditional equilibrium constant for the reaction of an inclusion complex with a saccharide.

Results and discussion

Probes **1** and **2** were synthesised by amide condensation of 1-aminopyrene and a corresponding carboxylbenzoxaborole precursor (Scheme 1), and identified by ^{1}H NMR, ^{13}C NMR, and high-resolution electrospray mass spectral measurements (Fig. S1†).

The UV-vis absorption and fluorescence spectra of **1** and **2** were measured in DMSO/water (2/98 in v/v, Fig. S2 and S3†) in the presence of β-cyclodextrin (β-CyD) and γ-CyD. All spectra were measured in the same solvent system unless otherwise noted. In the presence of β-CyD, both UV-vis absorption spectra of **1** and **2** exhibited absorption bands at 280 and 340 nm, which were assigned to an admixture of π–π* transition (pyrene) with intramolecular charge transfer (benzoxaborole → pyrene) and π–π* transition (pyrene), respectively, according to time-dependent density-functional theory (TD-DFT) calculations (Fig. S4 and Table S1†). Both **1** and **2** with β-CyD exhibited a broad fluorescence spectrum centred at approximately

430 nm. Because β-CyD forms a 1 : 1 inclusion complex that encapsulates one molecule of a pyrene compound, the UV-vis absorption and fluorescence spectra of **1** and **2** with β-CyD are ascribed to each monomeric probe encapsulated by β-CyD. In contrast, in the presence of γ-CyD, the UV-vis absorption spectra of **1** and **2** showed bathochromic shifts compared with the spectra observed in the presence of β-CyD. This bathochromic shift is ascribed to the formation of pyrene dimer with J-aggregation-like structure in the γ-CyD cavity; the two molecules of the probes in the cavity overlap each other with a slight shift from the completely overlapping position.[14] The fluorescence spectra of **1** and **2** with γ-CyD exhibited a band at 500 nm in addition to the monomeric fluorescence at 430 nm. These results indicate that γ-CyD encapsulates two molecules of the probes inside its cavity to form the pyrene dimer, which exhibits dimeric fluorescence at 500 nm. The assignments are supported by the induced circular dichroism (ICD) spectral study discussed below. **1** with γ-CyD showed a larger bathochromic shift of the UV-vis absorption spectrum and a stronger dimeric fluorescence than **2** with γ-CyD, suggesting that **1** forms a dimer inside the γ-CyD cavity more efficiently than **2**. To obtain further evidence for the structure of the inclusion complexes, nuclear Overhauser effect spectroscopy (NOESY) spectrum of **1** with γ-CyD was measured (Fig. S5†). The spectra showed cross-peaks between aromatic protons of **1** and the H3 proton of γ-CyD, clearly indicating that **1** was encapsulated by γ-CyD.

The UV-vis absorption spectra of the inclusion complexes of γ-CyD with a dimer of **1** and **2** (hereinafter referred to as **1/γCyD** and **2/γCyD**, respectively) were measured under various pH conditions (Fig. S6†). The pK_a^{B} values of **1/γCyD** and **2/γCyD** were determined to be 6.41 ± 0.14 and 6.56 ± 0.12, respectively. This indicates that both **1/γCyD** and **2/γCyD** possess higher acidities than typical phenylboronic acid derivatives (pK_a^{B} = 7–9)[18] so that tetrahedral boronate ion species is predominant at physiological pH (= 7.4). The pH dependence of the UV-vis absorption spectra of **1/γCyD** with various saccharides (D-fructose, D-glucose, D-galactose, and D-allulose) revealed that the apparent pK_a^{B} of **1/γCyD** was decreased in the presence of 30 mM saccharides (Fig. S7†): 5.25 ± 0.06 (D-fructose), 6.11 ± 0.09 (D-glucose), 6.26 ± 0.09 (D-galactose), and 4.60 ± 0.16 (D-allulose), implying that the order of the affinity of the saccharides for **1/γCyD** is D-allulose > D-fructose > D-galactose ≈ D-glucose.[19] A similar trend was observed for **2/γCyD** (Fig. S7 and Table S2†).

Fig. 1 shows the fluorescence spectra of **1/γCyD** in the absence and presence of 1 mM of saccharides. The intensity of monomeric fluorescence of **1/γCyD** at 430 nm hardly changed by the addition of saccharides, whereas the intensity of dimeric fluorescence of **1/γCyD** at 500 nm decreased when D-allulose and D-fructose were added. This feature allows **1/γCyD** to detect D-allulose and D-fructose ratiometrically with the fluorescence intensities at 430 and 500 nm. In contrast, the intensity of dimeric fluorescence of **2/γCyD** at 500 nm slightly increased by the addition of saccharides (Fig. S8†), suggesting that **1/γCyD** and **2/γCyD** recognise saccharides through different sensing mechanisms.

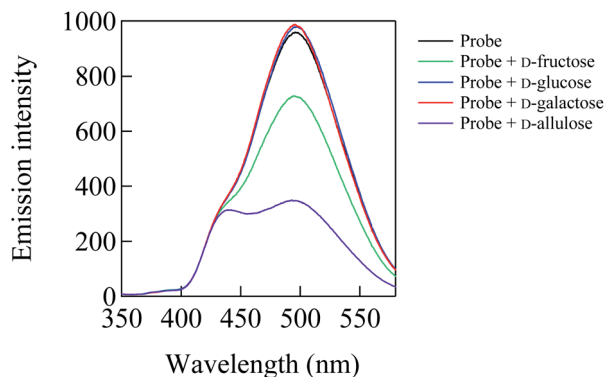**Fig. 1** Fluorescence spectra of **1/γCyD** in the absence (black) and presence of each saccharide (1 mM) in DMSO/water (2/98 in v/v): $C_{probe} = 10.7$ μM, $C_{γCyD} = 5$ mM, 10 mM of phosphate buffer, pH = 7.4, $T = 25\ ^{\circ}C$, $I = 0.10$ M, and $\lambda_{ex} = 305$ nm.

The fluorescence spectra of **1/γCyD** and **2/γCyD** were measured under various pH conditions in the absence and presence of saccharides (Fig. S9†). The intensities of monomeric and dimeric fluorescence remained unchanged and decreased as the solution pH was decreased, respectively, for both **1/γCyD** and **2/γCyD** in the absence of saccharides. The same trend was noted in the presence of saccharides. **1/γCyD** showed larger changes in the intensity ratios of dimeric fluorescence at 500 nm to monomeric fluorescence at 430 nm (I_{500}/I_{430}) by the addition of saccharides than **2/γCyD** (Fig. S10†) at pH 7.4, indicating that **1/γCyD** is superior to **2/γCyD** as a saccharide chemosensor.

Fig. 2 shows I_{500}/I_{430} of **1/γCyD** at pH 7.4 under various concentrations of each saccharide. I_{500}/I_{430} decreased when the saccharide concentration was increased. The decrease in I_{500}/I_{430} by the addition of D-glucose and D-galactose was much
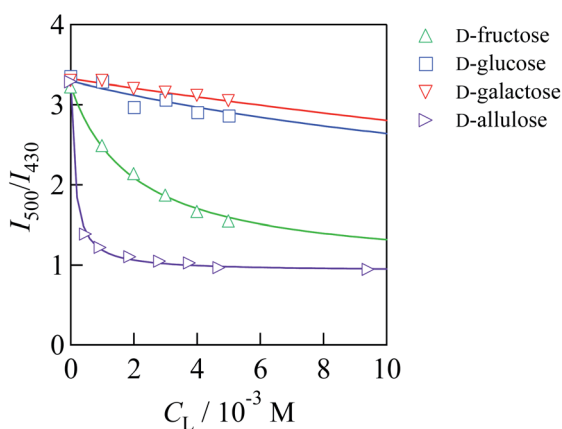
smaller than that by the addition of D-fructose, in agreement with the affinity of the saccharides for monoboronic acid.[12] This suggests that each boronic acid moiety of **1/γCyD** recognises saccharides in 1 : 1 stoichiometric ratio. The conditional equilibrium constants (K's) for the binding of **1/γCyD** with saccharides were determined by applying non-linear least squares fitting to a theoretical equation derived from the 1 : 1 binding model (eqn (1)), and the values were $498 \pm 35\ M^{-1}$ for D-fructose, $48.4 \pm 25.3\ M^{-1}$ for D-glucose, $15.0 \pm 3.3\ M^{-1}$ for D-galactose, and $(8.05 \pm 0.59) \times 10^3\ M^{-1}$ for D-allulose (Fig. S11†). These results demonstrate that **1/γCyD** possessing benzoxaborole moieties has much higher affinity for D-allulose than D-fructose, consistent with the previous report of Arimitsu et al.[11] Competition experiments showed that **1/γCyD** selectively recognised D-allulose in the presence of the other saccharides (Fig. S12†). From the calibration curve for the quantification of D-allulose by **1/γCyD** at pH 8.0, the limits of detection and quantification were determined to be 6.9 and 21 μM, respectively (Fig. S13†). Fig. 3 shows the fluorescence colours of **1/γCyD** in the absence and presence of 1 mM saccharides. **1/γCyD** exhibited no observable change in fluorescence colour by the addition of D-fructose, D-glucose, and D-galactose. In contrast, the fluorescence colour of **1/γCyD** changed from green to blue in the presence of D-allulose. These results demonstrate that **1/γCyD** enables highly selective and sensitive detection of D-allulose by the naked eye. Both D-fructose and D-allulose are known to form five isomers in aqueous solution (Scheme S2†). Of these isomers, the reactive species for each reaction with boronic acids is β-D-fructofuranose for D-fructose and α-D-allulofuranose for D-allulose, which accounts for 22% and 39% of the total isomers in solution, respectively; boronic acids bond to hydroxyl groups at the 2-, 3- and 6-positions of β-D-fructofuranose and the 2- and 3-positions of α-allulofuranose to form cyclic boronate ester ions.[11,20] Therefore, the higher affinity of D-allulose for boronic acids than D-fructose is caused by the larger abundance of the reactive species in the case of D-allulose. Because of the low water solubility of **2/γCyD** and the small
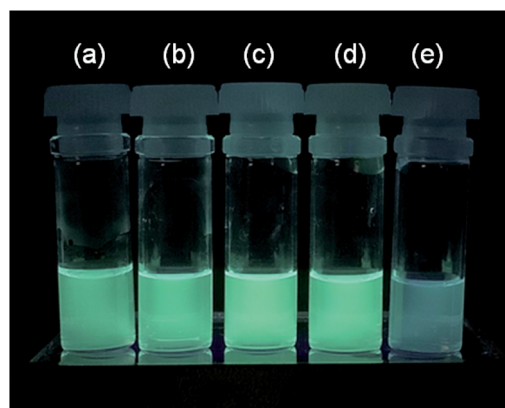

Fig. 2 Ratio of fluorescence intensities at 500 and 430 nm (I_{500}/I_{430}) of **1/γCyD** at various concentrations of each saccharide in DMSO/water (2/98 in v/v): $C_{probe} = 10.7$ μM, $C_{γCyD} = 5$ mM, 10 mM of phosphate buffer, pH = 7.4, $T = 25\ ^{\circ}C$, $I = 0.10$ M, and $\lambda_{ex} = 305$ nm. Each solid curve indicates a theoretical curve derived from the 1 : 1 binding model fitted by non-linear least squares analysis using the data obtained at $C_{saccharide} = 0$–30 mM for each reaction system. All data are shown in Fig. S11.†

Fig. 3 Photograph of fluorescence of **1/γCyD** in the absence (a) and presence of 1 mM of D-fructose (b), D-glucose (c), D-galactose (d), and D-allulose (e) in DMSO/water (2/98 in v/v) at room temperature with 365 nm UV light: $C_{probe} = 10.3$ μM, $C_{γCyD} = 5$ mM, 10 mM of phosphate buffer, pH = 7.4, and $I = 0.10$ M.

change in fluorescence spectra by the reaction with saccharides, the K' values for the reactions of **2/γCyD** with saccharides were unable to be precisely determined. Furthermore, little change in fluorescence colour was observed by the addition of saccharides (Fig. S14†). These results indicate that **2/γCyD** is unsuitable for saccharide sensing.

The ICD spectra were measured to elucidate the sensing mechanisms of **1/γCyD** and **2/γCyD** for saccharides. Fig. 4 shows the ICD spectra of **1/γCyD** in the absence and presence of saccharides. The ICD spectrum of **1/γCyD** exhibited a bisignate Cotton effect, indicating that γ-CyD simultaneously encapsulates two molecules of **1** to form a chiral inclusion complex. Because this spectrum showed a positive first Cotton effect at approximately 410 nm and a negative second Cotton effect at 360 nm, two molecules of **1** would be encapsulated in γ-CyD in the clockwise direction.[21,22] Distinct bisignate signals were visible in the 250 to 290 nm region, where an absorption band ascribed to intramolecular charge transfer with the participation of the electron orbital of the benzoxaborole moieties appeared. This suggests that γ-CyD encapsulates not only the dimeric pyrene moieties of the two molecules of **1**, but also the two benzoxaborole moieties to form a 2 : 2 stoichiometric inclusion complex. The addition of ᴅ-glucose and ᴅ-galactose produced no observable changes in the ICD spectrum of **1/γCyD**. In contrast, the bisignate signals in the spectrum disappeared by the addition of ᴅ-allulose and ᴅ-fructose, resulting in a spectrum with a positive Cotton effect at 350 nm and weak negative Cotton effect at 310 nm in the presence of ᴅ-allulose. This spectral change indicates that one of the two molecules of **1** is released from the γ-CyD cavity to form the 1 : 1 stoichiometric inclusion complex by the reaction with ᴅ-allulose and ᴅ-fructose. Therefore, the diminishment of the dimeric fluorescence of **1/γCyD** by the reactions with ᴅ-allulose and ᴅ-fructose originates from the monomerisation of dimeric **1/γCyD**, as shown in Scheme 2. The monomerisation is caused by the bulkiness of the saccharides that bind to the benzoxaborole moieties of **1/γCyD**. Consequently, the change from dimeric to monomeric fluorescence enables ratiometric fluorescence
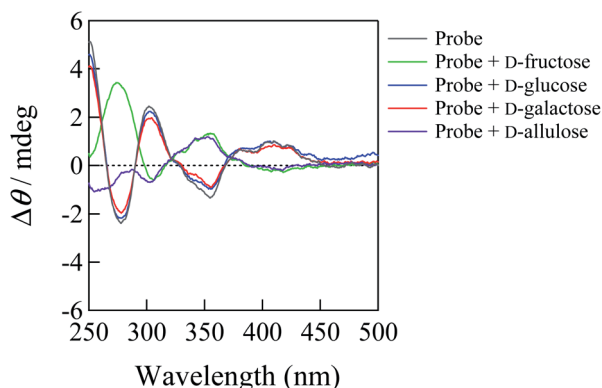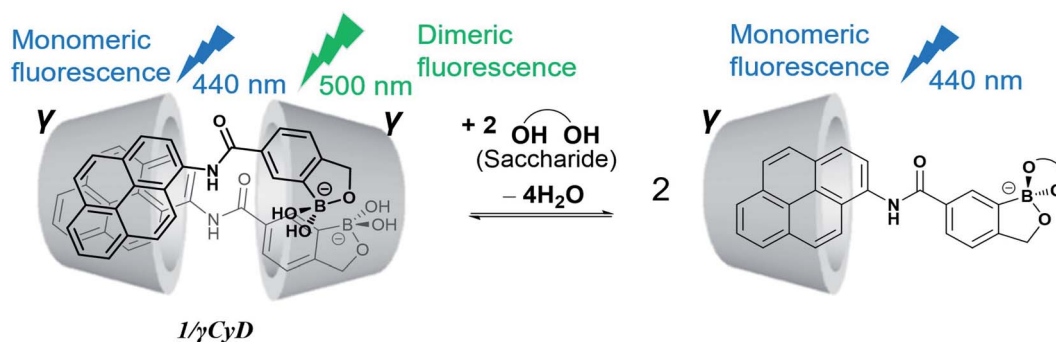

Fig. 4 ICD spectra of **1/γCyD** in the absence and presence of each saccharide (10 mM) in DMSO/water (2/98 in v/v): $C_{probe} = 10.3$ μM, $C_{γCyD} = 5$ mM, 10 mM of phosphate buffer, pH = 10.2, $T = 25$ °C, and $l = 0.10$ M.

sensing of ᴅ-allulose. It should be noted that, in the ICD spectrum of **1/γCyD**, the strong positive Cotton effect observed at 280 nm in the presence of ᴅ-fructose and the weak negative Cotton effect observed at 260 nm in the presence of ᴅ-allulose are ascribed to ᴅ-fructose and ᴅ-allulose themselves, respectively (Fig. S15†).[23] In contrast, the ICD spectrum of **2/γCyD** showed a spectrum with a negative first Cotton effect at approximately 410 nm and a positive second Cotton effect at 360 nm, indicating that two molecules of **2** are encapsulated inside the γ-CyD cavity in the counterclockwise direction (Fig. S16†). Because the ICD spectrum of **2/γCyD** shows weak peaks in the 250 to 290 nm region, the 2 : 1 stoichiometric inclusion complex of **2** with γ-CyD possibly forms without the encapsulation of the benzoxaborole moieties by γ-CyD. The peaks in the ICD spectrum of **2/γCyD** were slightly intensified by the reaction with saccharides, probably due to the formation of stable chiral complex through hydrogen bonding interactions between the free hydroxyl groups of the saccharide moieties (Scheme S3†). Hence, the low sensitivity of **2/γCyD** to saccharides would be ascribed to the small structural change of **2/γCyD** by the reaction with saccharides.

The boron centre of **2** is located at the *para*-position from the amide group, so that the two benzoxaborole moieties of **2** are hardly encapsulated by γ-CyD because the anionic boronate moieties of **2/γCyD** face the hydrophobic γ-CyD cavity when γ-CyD approaches the benzoxaborole moieties. In contrast, because the boron centre of **1** is located at the *meta*-position from the amide group, the anionic boronate moieties of **1** can face inward so that the two benzoxaborole moieties are encapsulated by the γ-CyD cavity (Scheme 2). Because the γ-CyDs of **1/γCyD** hold the two benzoxaborole moieties as well as the pyrene moieties, the motion of the two molecules of **1** are rigidified to enhance the fluorescence intensity. This explains that **1/γCyD** exhibits stronger intensity of dimeric fluorescence than **2/γCyD**.

The sensing mechanism of **1/γCyD** for ᴅ-allulose in Scheme 2 is also supported by UV-vis absorption spectral study. As the ᴅ-allulose concentration was increased, the UV-vis absorption spectrum of **1/γCyD** showed slight hypsochromic shift and increase in the absorbances at 327 and 342 nm (Fig. S11-5b†), namely, the UV-vis absorption spectra approached the spectrum of **1** in the presence of β-CyD (Fig. S2-1†). This suggests that the 1 : 1 stoichiometric inclusion complex is formed by the reaction with ᴅ-allulose.

The optimal pH (pH$_{opt}$) at which the reaction of a boronic acid with a saccharide proceeds most efficiently is known to be the average value of pK_a^B and pK_a of the saccharide (pK_a^L), *i.e.*, (pK_a^B + pK_a^L)/2.[18] Those pK_a values are typically $7 < pK_a^B < 10$ and $pK_a^L > 12$. Many conventional boronic acid-based chemosensors utilise the structural change of the boronic acid moiety from trigonal to tetrahedral boron centre to produce ratiometric fluorescence response. However, the reaction of boronic acids with saccharides hardly proceeds under the conditions where the trigonal boronic acid species is predominant (pH < pK_a^B < pH$_{opt}$) because the pH is far from the pH$_{opt}$. Whereas boronic acids react with saccharides efficiently at around the pH$_{opt}$ where tetrahedral boronate ion is predominant (pK_a^B < pH ≈ pH$_{opt}$), ratiometric fluorescence response is hardly produced

Scheme 2 Plausible mechanism for sensing saccharides by **1/γCyD**.

because of the small structural change of the boronic acid moiety from tetrahedral boronate ion to tetrahedral boronate ester ion (Scheme S4a†). This study demonstrates that **1/γCyD** utilises the monomerisation of the dimeric probe that is encapsulated by γ-CyD as a novel sensing mechanism for saccharides. Because **1/γCyD** ($pK_a^B = 6.41$) has more acidic boronic acid moiety compared with typical phenylboronic acid-based chemosensors ($pK_a^B = 7–10$), the pH_{opt} for the reaction of **1/γCyD** with saccharides approaches 7.4. Resultantly, **1/γCyD** binds efficiently to the *cis*-diol moiety of D-allulose at the physiological pH. Therefore, this system enables ratiometric fluorescence sensing of D-allulose at pH 7.4 with high sensitivity owing to the tetrahedral boronate ion species of **1/γCyD** that shows ratiometric fluorescence response to saccharides (Scheme S4b†). Many reported mono-boronic acid-based chemosensors were evaluated as sensors for D-fructose owing to its high affinity for mono-boronic acids. In contrast, we have demonstrated that the boronic acid-based chemosensors in this study selectively recognise D-allulose rather than D-fructose by exploiting the higher affinity of boronic acids for D-allulose than D-fructose. Therefore, this study provides novel insights into the research area of boronic acid-based molecular recognition to design chemosensors for the rare sugar.

Conclusions

We have reported **1/γCyD** as a novel fluorescence chemosensor that can detect D-allulose ratiometrically with high sensitivity and selectivity by applying benzoxaborole moieties to the reaction sites. On the basis of the monomerisation of the dimeric **1/γCyD** by the reaction with D-allulose, we have uncovered a novel sensing mechanism that enables the visual detection of D-allulose. Unlike many boronic acid-based chemosensors for saccharides, **1/γCyD** can work in a water-rich solvent by exploiting the feature of γ-CyD that solubilises hydrophobic probes in water. Furthermore, **1/γCyD** detects D-allulose at physiological pH with ratiometric fluorescence response, which enables accurate detection of the target molecule. According to the calibration curve of **1/γCyD** for the quantification of D-allulose, the linear relationship holds between I_{500}/I_{430} and D-allulose concentration from 0 to 50 μM (Fig. S13†). Considering that the limits of detection and quantification are 6.9 and 21

μM, respectively, **1/γCyD** can detect and quantify D-allulose at the μM level. In addition, excellent selectivity of **1/γCyD** for D-allulose was observed (Fig. S12-2†). This allows specific detection of D-allulose in biological and food samples containing various saccharides. Furthermore, because **1/γCyD** is based on artificial molecules, it possesses much higher stability against heat and pH compared to enzyme-based biosensors. This feature enables accurate and reproducible measurements for the determination of D-allulose concentration. These attractive features indicate that **1/γCyD** has utility as a D-allulose chemosensor in broad fields such as industry, biology, and medicine. Therefore, **1/γCyD** is a potential candidate not only for the sensing system of D-allulose but also for the analysis of dynamics in the human body and the collection systems of the rare sugar.

Conflicts of interest

There are no conflicts to declare.

Acknowledgements

Notes and references

1 NCD Risk Factor Collaboration (NCD-RisC), *Lancet*, 2016, **387**, 1513–1530.

2 S. Wild, G. Roglic, A. Green, R. Sicree and H. King, *Diabetes Care*, 2004, **27**, 1047–1053.

3 C. D. Mathers and D. Loncar, *PLoS Med.*, 2006, **3**, 2011–2030.

4 T. Matsuo, H. Suzuki, M. Hashiguchi and K. Izumori, *J. Nutr. Sci. Vitaminol.*, 2002, **48**, 77–80.

5 S. Jiang, W. Xiao, X. Zhu, P. Yang, Z. Zheng, S. Lu, S. Jiang, G. Zhang and J. Liu, *Front. Bioeng. Biotechnol.*, 2020, **8**, 26.

6 A. Hossain, F. Yamaguchi, T. Matsuo, I. Tsukamoto, Y. Toyoda, M. Ogawa, Y. Nagata and M. Tokuda, *Pharmacol. Ther.*, 2015, **155**, 49–59.

7 S. D. Bull, M. G. Davidson, J. M. H. van den Elsen, J. S. Fossey, A. T. A. Jenkins, Y. B. Jiang, Y. Kubo, F. Marken, K. Sakurai, J. Zhao and T. D. James, *Acc. Chem. Res.*, 2013, **46**, 312–326.

8 X. Wu, Z. Li, X. X. Chen, J. S. Fossey, T. D. James and Y. B. Jiang, *Chem. Soc. Rev.*, 2013, **42**, 8032–8048.

9 X. Sun and T. D. James, *Chem. Rev.*, 2015, **115**, 8001–8037.

10 Y. Nakagawa, H. Tateno and M. Ebara, *Chem. Lett.*, 2018, **47**, 134–137.

11 K. Arimitsu, H. Iwasaki, H. Kimura and H. Yasui, *Chem. Lett.*, 2021, **50**, 1470–1474.

12 J. A. Peters, *Coord. Chem. Rev.*, 2014, **268**, 1–22.

13 Y. Tsuchido, S. Fujiwara, T. Hashimoto and T. Hayashita, *Chem. Pharm. Bull.*, 2017, **65**, 318–325.

14 T. Hashimoto, M. Kumai, M. Maeda, K. Miyoshi, Y. Tsuchido, S. Fujiwara and T. Hayashita, *Front. Chem. Sci. Eng.*, 2020, **14**, 53–60.

15 J. Fan, M. Hu, P. Zhan and X. Peng, *Chem. Soc. Rev.*, 2013, **42**, 29–43.

16 C. Priem and A. Geyer, *Chem.–Eur. J.*, 2019, **25**, 14278–14283.

17 (*a*) M. C. L. Yeung, B. W. K. Chu and V. W. W. Yam, *ChemistryOpen*, 2014, **3**, 172–176; (*b*) A. Ito, S. Ishizaka and N. Kitamura, *Phys. Chem. Chem. Phys.*, 2010, **12**, 6641–6649.

18 M. A. Martínez-Aguirre, R. Villamil-Ramos, J. A. Guerrero-Alvarez and A. K. Yatsimirsky, *J. Org. Chem.*, 2013, **78**, 4674–4684.

19 G. Springsteen and B. Wang, *Tetrahedron*, 2002, **58**, 5291–5300.

20 (*a*) J. C. Norrild and H. Eggert, *J. Chem. Soc., Perkin Trans.*, 1996, **2**, 2583–2588; (*b*) K. Fukada, T. Ishii, K. Tanaka, M. Yamaji, Y. Yamaoka, K. Kobashi and K. Izumori, *Bull. Chem. Soc. Jpn.*, 2010, **83**, 1193–1197; (*c*) T. Barclay, M. Ginic-Markovic, M. R. Johnston, P. Cooper and N. Petrovsky, *Carbohydr. Res.*, 2012, **347**, 136–141.

21 K. Kano, H. Matsumoto, Y. Yoshimura and S. Hashimoto, *J. Am. Chem. Soc.*, 1988, **110**, 204–209.

22 N. Harada and N. Berova, in *Comprehensive Chirality*, ed. E. M. Carreira and H. Yamamoto, Elsevier, Amsterdam, 2012, vol. 8, pp. 449–477.

23 A. Kimura, S. Chiba and M. Yoneyama, *Carbohydr. Res.*, 1988, **175**, 17–23.